Desalination and Water Treatment
www.deswater.com

doi: 10.5004/dwt.2021.27667

236 (2021) 55–68
October

Polycyclic aromatic hydrocarbons removal from vehicle-wash wastewater using activated char

Muhammad Ilyas[a,*], Waqas Ahmad[b], Hizbullah Khan[a]

[a]*Department of Environmental Sciences, University of Peshawar, Peshawar, Khyber Pakhtunkhwa, Pakistan, Tel. +923078064028; emails: sirfilyas@yahoo.com (M. Ilyas), hizbullah@uop.edu.pk (H. Khan)*
[b]*Institute of Chemical Sciences, University of Peshawar, Peshawar, Khyber Pakhtunkhwa, Pakistan, email: waqasahmad@uop.edu.pk*

Received 17 March 2021; Accepted 30 July 2021

ABSTRACT

In this study, waste polyethylene terephthalate (wPET) and waste polystyrene (wPS) was converted into activated char (AC) and utilized for the removal of polycyclic aromatic hydrocarbons (PAHs) from vehicle-wash wastewater (VWW). AC was prepared by carbonization in nitrogen atmosphere at high temperature followed by chemical activation with 1 M KOH and HCl. The AC was investigated by surface area analyser, Fourier-transform infrared spectroscopy as well as scanning electron microscopy. The removal of PAHs from VWW through AC was examined by batch adsorption tests. Adsorption factors, including; initial PAHs concentration, contact time, temperature, and adsorbent dose were studied. The PAHs contents were measured by using a UV spectrometer and the adsorption efficiency was calculated under optimal conditions. Kinetic and isotherm models were applied to evaluate the adsorbents' capacity for PAHs adsorption. Kinetic studies have shown that the adsorption of these PAHs on AC follows pseudo-second-order kinetics. Experimental results show that both Langmuir and Freundlich isotherm models are most suitable for this data. The calculated thermodynamic factors such as entropy change ($\Delta S°$), enthalpy change ($\Delta H°$) and free energy change ($\Delta G°$) indicate that the adsorption process is essentially non-spontaneous and exothermic. This examination revealed that the novel AC presents a large potential in the PAHs elimination and recovery from VWW.

Keywords: Polycyclic aromatic hydrocarbons; Char; Vehicle-wash wastewater; Sorption experiments

1. Introduction

Polycyclic aromatic hydrocarbons (PAHs) are precedence organic toxins, which are pervasively occur in vegetation, soils, sediments, aquatic as well as atmospheric systems and consequently are firmly checked in the environment [1,2]. They are considerable groups of organic compounds with at least 2 or more fused aromatic rings having atomic masses in the range of 128 to 278 Daltons [3]. In the environment, there are thousands of PAH compounds, yet PAHs investigation is limited to a couple of compounds, mostly the 16 precedence compounds comprising benz(a)anthracene (BaA), naphthalene (Nap), phenanthrene (Ph), benzo(a)pyrene (BaP), fluorene (Fl), benzo(ghi)perylene (B[ghi]P), acenaphthene (Ace), acenaphthylene (Acy), benzo(b) fluoranthene (BbF), anthracene (Ant), fluoranthene (Flu), dibenz(ah)anthracene (D[ah]A), pyrene (Pyr), chrysene (Chr), indeno(123-cd)pyrene (InP) and benzo(k)fluoranthene (BkF) recorded by USEPA as possibly lethal [4]. The PAHs having four or more than four aromatic rings are more lipophilic, less volatile and are less water soluble than the PAHs with three aromatic rings [2]. Several of these PAHs are teratogenic, cancer-causing, genotoxic as well as mutagenic in nature with an extended range of transport and all

---

* Corresponding author.

1944-3994/1944-3986 © 2021 Desalination Publications. All rights reserved.

around embroiled in endocrine system disruption at higher levels [5].

PAHs are transported into the environment on account of common exercises, for example, volcanic activity, microbial synthesis, and terrestrial vegetation synthesis. Although, the PAHs released as a result of these processes is negligible in examination with those generated from anthropogenic sources, grass land as well as forest fires [6]. Manmade exercises (e.g., emissions from internal combustion engines, heating and power generation, coal tar pitch and asphalt, manufacturing of carbon black, leakage from the petroleum industry, residential waste burning, combustion of fossil fuels, agricultural production, vehicular emissions and military operations) discharge a lot of PAHs on the earth [7,8]. The cancer-causing nature of PAHs expanded with expanding subatomic weight [9]. Human introduction to PAHs has been related to an expanded danger of creating malignancy in an assortment of organs (e.g., pancreas, kidney, prostate, esophageal, breast, scrotum, larynx, skin, stomach, bladder and lung). Moreover, they suppress the immune system as well as are associated with being endocrine disrupters [10,11].

The general properties of PAHs are low aqueous solubility, high boiling as well as melting point, and low vapor pressure (in this manner they are solid). Generally, the latter two qualities will decrease with the increase of atomic weight. In fact, the oxidation resistance and reducibility will increase [12]. The PAHs solubility diminishes for every additional ring [12]. In the interim, PAHs are soluble in natural solvents because of their extraordinary lipophilicity. PAHs also show different capacities, for example, corrosion resistance, physiological action, conductivity, light sensitivity, and heat resistance [13]. However, some PAHs have some commercial uses. They are generally utilized as intermediaries in chemical industries, lubricating materials, photographic products, agricultural products, and pharmaceuticals [14]. Although, the overall uses of a number of PAHs are [15]:

- Ace: production of pharmaceuticals, pesticides, dyes, as well as pigments.
- Pyr: manufacture of pigments.
- Ant: diluent for wood preservatives in addition to production of pigments as well as dyes.
- Flu: manufacture of pharmaceuticals, dyes as well as agrochemicals.
- Fl: production of dyes, pesticides, pigments as well as pharmaceuticals.
- Ph: production of pesticides as well as resins.

Other PAHs may be contained in asphalt, used for the construction of roads, in addition to roofing tar. Furthermore, specific refined products, of precise PAHs, are used also in the field of liquid crystals and electronics.

Due to the carcinogenic, mutagenic, as well as toxic qualities of PAHs, noteworthy enthusiasm for creating suitable expulsion measure through understanding remediation systems has been raised [16]. In order to reduce the potential dangers of PAHs to the environment and human well-being, various techniques have been explored to eliminate PAHs from water-polluted soils. Various techniques have been explored to eliminate PAHs from sullied soils in addition to waters to alleviate the conceivable danger of PAHs on the environment as well as human wellbeing [17]. In any case, most of these strategies have some obstacles, for example, confused working systems, high support, and venture costs. In addition, some of these treatments can play an auxiliary role, some of which are mutagenic and carcinogenic (such as trihalomethanes, halogenated citric acid) mixtures, and further include adverse effects and general health conditions [18]. However, among these techniques, the adsorption cycle appears to hold guarantee for the expulsion of organic and inorganic micro-pollutants in a conservative and natural amicable way [19,20]. Variety of adsorbents used for this purpose include biochar/bentonite/waste polystyrene and biochar/bentonite/waste polyethylene terephthalate [19,21], L-cysteine-modified montmorillonite-immobilized alginate nanocomposite [22], poly (methyl methacrylate)-grafted alginate/Fe_3O_4 nanocomposite [23], montmorillonite clay [24], green synthesis of silver nanoparticles [25], iron oxide-impregnated dextrin nanocomposite [26], papaya peel carbon [27], chitosan grafted polyaniline [28], waste rubber tires [29], iron-based metal organic framework [30], a non-carbon adsorbent nano alumina [31], various adsorbents for caffeine, nicotine and amoxicillin [32], Fe-benzene dicarboxylic acid metal organic framework [33], ZnNiIn layered double hydroxides derived mixed metal oxides [34], and hen feather [35]. Consequently, few investigations have been completed to locate the viable and monetary sorption media and natural components influencing the PAHs expulsion measures [36,37]. The fundamental objective of this examination is the utilization of wPS and wPET in the synthesis of modified AC using KOH to increase the functionality and porosity of the synthesized materials for removing the PAHs from vehicle-wash wastewater (VWW). The process for preparation of AC is a relatively low-cost and effective method since an alternative source as wPS and wPET is utilized. Furthermore, various trial conditions were set to identify their effects and explore the ideal removal performance of AC.

2. Experimental setup

2.1. Sample collection and preparation

The VWW samples from both heavy and light vehicle-wash stations (trailers, buses, pickups, cars, etc.) were collected and homogenized in precleaned 2.5 L amber glass bottles. The waste plastic collection and preparation detail is given in our previous paper [19]. The samples were shipped to the Laboratory Department of Environmental Sciences, University of Peshawar.

2.2. AC preparation and characterization

The wPS and wPET materials were carbonized in nitrogen at 600°C. Distilled water and HCl solution (1 M) were used to wash the obtained solids in order to reduce the decomposed fragments and ash and then dried for 24 h at 110°C. The obtained AC were ground and screened through a sieve, with pore size 250 μm [38]. The AC were characterized by specific surface area analysis (NOVA2200e, Quantachrome, USA), FT-IR (Spectrum Two, S.No: 103385) analysis as well as SEM (JSM-5910, JEOL, Japan).

2.3. Adsorption experiments

Adsorption of PAHs from VWW over wPET-AC and wPS-AC was studied in batch mode adsorption experiments. Several variables were measured in the study, including dosage of AC (0.2, 0.4, 0.6, and 0.8 g/100 mL), contact time (0.25, 0.5, 1, and 2 h) and PAHs concentrations (10, 20, 30, and 40 ppm). 100 mL of samples were used throughout the experiment. All adsorption and kinetic models of PAHs were performed using 500 mL Erlenmeyer flasks at various temperatures in a batch system. Samples were mixed in a magnetic stirrer with 150 rpm at various temperatures (20°C, 30°C, 40°C, 50°C) until equilibrium was reached.

2.4. Analyses and calculations

The equilibrium concentration, q_e (μg g^{-1}) and % q_e was calculated as per Table 1.

The data were fitted to the numerical models introduced in Table 2. All tests were conducted on the 16-PAHs individually. UV-Vis spectrophotometry (Shimadzu UV-1700, Japan) was used to determine the concentration of PAHs in the solution and VWW [43]. The concentrations of physical and biochemical parameters such as pH, suspended solids, total dissolved solids (TDS), chemical oxygen demand (COD), dissolved oxygen (DO), biological oxygen demand (BOD$_5$), turbidity, colour, and odour were determined by similar methods as given in our past paper [44].

Table 1
Equations used for q_e and % q_e calculations

	Equation	
Equilibrium concentration	$q_e = \frac{\left[\left(C_0 - C_i\right)V\right]}{M}$	(1)
	where, C_0 (μg L^{-1}) = Initial PAHs concentration C_i (μg L^{-1}) = Equilibrium PAHs concentration V (L) = Volume of solution M (g) = Mass of AC	
Percentage removal	$\% q_e = \frac{\left[\left(C_0 - C_i\right) \times 100\right]}{C_0}$	(2)

Table 2
Adsorption models used in the study

Model	Equation	
Kinetic models		
Pseudo-first order [39]	$\ln\left(q_e - q_t\right) = \ln q_e + k_1 t$	(3)
	where, q_e = equilibrium sorption capacity (μg g^{-1}), q_t = sorption capacity (μg g^{-1}) at time t (h), k_1 = adsorption rate constant for pseudo-first order.	
Pseudo-second order [40]	$\frac{t}{q_t} = \frac{t}{q_e} + \frac{1}{k_2 q_e^2}$	(4)
	k_2 = adsorption rate constant for pseudo-second order.	
Equilibrium models		
Freundlich [41]	$\ln q_e = \ln K_f + \frac{1}{n} \ln C_e$	(5)
	$1/n$: measure of intensity of adsorption and K_f = Freundlich adsorption coefficient. n = Freundlich constant, C_e (μg L^{-1}) = equilibrium concentration of adsorbate q_e: amount of adsorbate adsorbed per unit mass of adsorbent (μg g^{-1}).	
Langmuir [42]	$\frac{C_e}{q_e} = \frac{1}{KQ_{\max}} + \frac{C_e}{Q_{\max}}$	(6)
	K = Langmuir constant relates the energy of adsorption q_m = maximum amount of PAHs adsorbed per unit mass of adsorbent (μg g^{-1}), q_e = amount of adsorbate per mass unit of adsorbent at equilibrium (μg g^{-1}), C_e = equilibrium concentration (μg L^{-1})	

3. Results and discussion

Initially, the time to remove PAHs by AC test was 1 h, and the ratio of adsorbent to solution was 0.3 g/100 mL at a temperature of 24°C ± 2°C. Fig. 1 shows the removal percentage of 16-PAHs. Further trials were directed under various conditions to examine the ideal adsorption parameters.

3.1. Properties of AC

The wPS-AC and wPET-AC prepared in the laboratory were described by FT-IR, SEM in addition to specific surface area analysis. Detailed discussion on the results is given in Table 3. The SEM micrograph of wPS-AC displays a rough and irregular morphology with numerous cavities and mounds on the surface. The SEM micrographs of

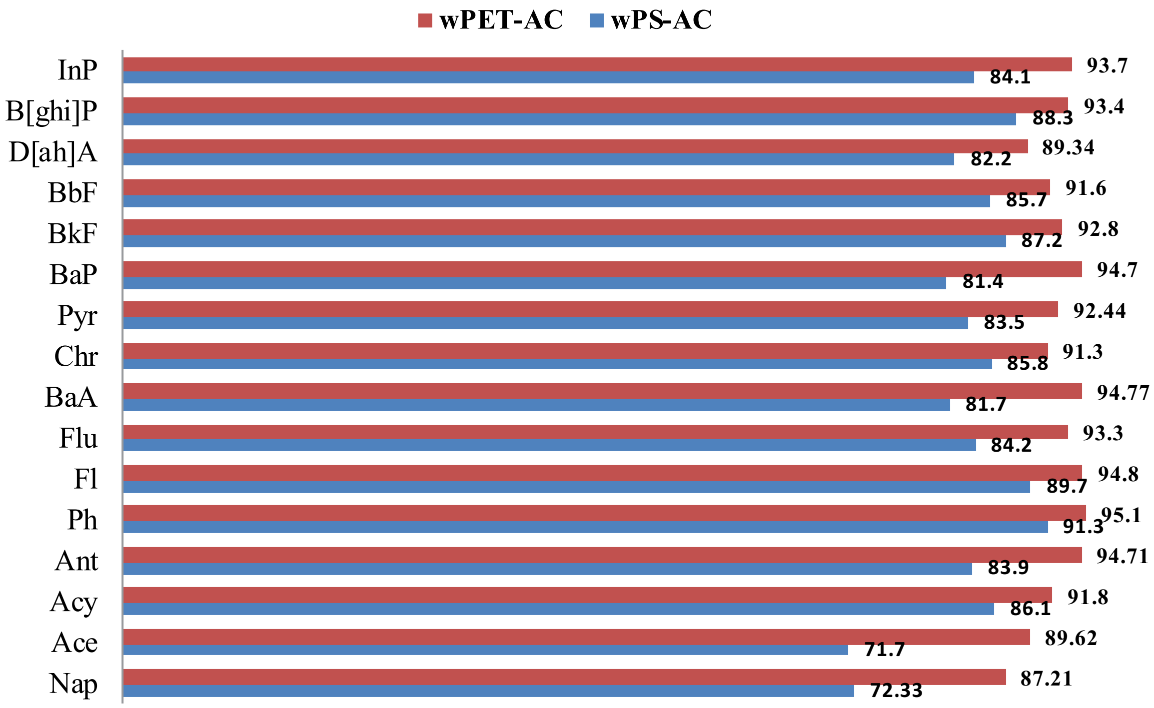

Fig. 1. % Removal efficiency of AC derived from wPET-AC and wPS-AC for 16-PAHs from VWW.

Table 3
SEM, FT-IR and surface area of wPET-AC and wPS-AC adsorbents

SEM analysis	FT-IR spectra	Surface area analysis
	wPET-AC	
- Dispersion of KOH particles over the surface of wPET-AC - Porous and rough surface structure - Presence of micropores	Absorption peaks at: - 3,414 cm^{-1} which might be due to stretching vibrations of –OH - 1,696 cm^{-1} (C=O, stretch) - 1,260 cm^{-1} (C=C, stretch) - 1,092 cm^{-1} (C–O, stretching vibration) - 1,010 cm^{-1} (C–O–C, stretching) - 720 cm^{-1} (C–H, stretch) and 521 cm^{-1} (C–H, stretch)	BJH surface area (m^2 g^{-1}): 11.02 BET surface area (m^2 g^{-1}): 65.35 R_p (A^0): 15.02 V_t (cm^3 g^{-1}): 0.009
	wPS-AC	
- Irregular fiber-like morphology - Rough surface - Spherical carbon black structure - Large macropores	The absorption bands were detected at: - 3,028 cm^{-1} (C–H, stretching) - 1,599 cm^{-1} (C=C, stretching) - 1,451 cm^{-1} (CH_2 stretching) - 1,017 cm^{-1} (C–O, stretching) - 696 cm^{-1} (C–H, stretching) and - 540 cm^{-1} (C–H, stretching).	BJH surface area (m^2 g^{-1}): 14.68 BET surface area (m^2 g^{-1}): 50.14 R_p (A^0): 14.09 V_t (cm^3 g^{-1}): 0.010

wPET-AC show a stretched but uneven morphology, with some fine particles agglomerated on the surface. The SEM analysis suggests that wPET-AC exhibits better porosity than wPS-AC. The new wPET-AC and wS-AC had functional groups of waste polymers, and therefore its adsorption efficiency was considered better than that of waste polymer. The surface properties, that is, BJH surface area (SBJH), BET surface area (SBET), pore volume, and pore radius of the AC, were determined using N_2 adsorption isotherms at 77.35 K. The results are given in Table 3. The results of surface analysis (Table 3) indicate that in case of wPET-AC and wPS-AC the calculated S_{BJH} was found to be 11.02 and 14.68 $m^2 g^{-1}$, the S_{BET} was 65.35 and 50.14 m^2g^{-1}, with pore radius of 15.02 A^0 and 14.09 A^0 and pore volume of 0.009 and 0.010 $cm^3 g^{-1}$, respectively. It is clear from the data that the AC possesses a high surface area and large pore dimensions than the waste polymers. Hence, the AC hold better adsorption potential compared with the waste polymers.

3.2. Batch experiments

3.2.1. Effect of adsorption dose

In adsorption studies, the dose of adsorbent is known to have an incredible effect. The amount of adsorbent that can be absorbed in the solution determines the number of active binding sites available for contaminants [45]. The effect of adsorbent dosage on the adsorption of PAHs onto wPS-AC and wPET-AC from VWW is shown in Figs. 2a and b, respectively. It was observed that as the adsorbent dose increased, the PAHs removal expanded. This swelling is attributed to the increase in the number of active sites that PAHs can bind and the increase in the adsorbent dosage. For an adsorbent dose of 0.8 g, the maximum adsorption percentage of PAHs was achieved, and after this stage, the adsorption proved to be practically consistent. With the increase of the adsorbent dosage, the increase of PAHs excretion percentage may be related to the increase of adsorbent surface area and adsorption site accessibility. As clear from the data, the maximum percentage removal of PAHs was attained for an adsorbent dose of 0.8 g, and after this stage the adsorption became almost constant. Similar behaviour has been observed in previous studies and arises from the effect of interactions between the adsorbate and adsorbent. The increased dose is consistent with the greater area and larger number of adsorption sites [37,46]. Therefore, due to its higher adsorption limit, a dose of 0.8 g of adsorbent was selected in this examination.

3.2.2. Effect of contact time

Considering that the adsorption rate is one of the compelling components that must be considered before designing the adsorption framework, a time-related check was performed. Figs. 2c and d show the adsorption of PAHs on wPS-AC and wPET-AC over time, respectively. The outcomes demonstrated that with expanding contact time there is an increase in the percentage removal. The reason behind the higher removal with expanding contact time is PAHs availability to adsorb over the surface of adsorbents. After 2 h of contact time, most of the active sites of the adsorbent are involved and equilibrium is reached. An equilibration time of 2 h was used in this examination to ensure the removal of PAHs.

3.2.3. Effect of temperature

The effect of solution temperature on the removal rate of PAHs in the solution on wPS-AC and wPET-AC is shown in Figs. 2e and f, respectively. With the increase of temperature, the removal of PAHs has been expanded. This indicates that the adsorption cycle is an endothermic cycle. As the temperature rises, the contaminant gains greater vitality, which breaks the vitality boundary between the contaminant and the AC. At the same time, due to the separation of some surface fragments on the AC, more vitality is produced on the surface of the adsorbent [47].

The spontaneity, thermal effect as well as feasibility of the adsorption system are determined by the change of the thermodynamic equilibrium constant K_D with temperature. Thermodynamic factors, for example, the entropy change ($\Delta S°$), free energy change ($\Delta G°$) as well as enthalpy change ($\Delta H°$) were determined by means of the following equations [48]:

$$\Delta G° = -RT \ln K_D \tag{7}$$

where R is the ideal gas constant, 8.314 J K^{-1} mol^{-1}; T is the absolute temperature in K; K_D is the equilibrium coefficient of the PAH adsorption on the AC.

$$\Delta H° = R \frac{T_2 T_1}{T_2 - T_1} \ln \frac{k_2}{k_1} \tag{8}$$

$$\Delta S° = \frac{\Delta H° - \Delta G°}{T} \tag{9}$$

The values of $\Delta G°$, $\Delta S°$ and $\Delta H°$ are shown in Table 4. The positive values of $\Delta G°$ and $\Delta S°$ indicate non-spontaneous processes. The negative value of $\Delta H°$ indicates the exothermic nature of the adsorption process.

3.2.4. Effect of initial concentration of PAHs on the adsorption process

The ability of wPS-AC and wPET-AC to remove PAHs from the VWW at various initial concentrations was also determined and shown in Figs. 2g and h, respectively. As an increase in the take-up limit with respect to PAHs with increment in initial concentration was acquired, this sorption trend showed that surface saturation is an element of the initial concentration in solution. The reason behind this pattern is that, at lesser concentration, less PAHs are accessible in solution, accordingly the maximum binding of the PAHs on the active sites of wPS-AC and wPET-AC was not accomplished, however as the concentration increases, the presence of a high concentration gradient produces a more grounded main impetus, which overcomes the resistances to mass exchange, simultaneously, utilizing the active sites bringing about higher adsorption per unit mass of wPS-AC and wPET-AC [49].

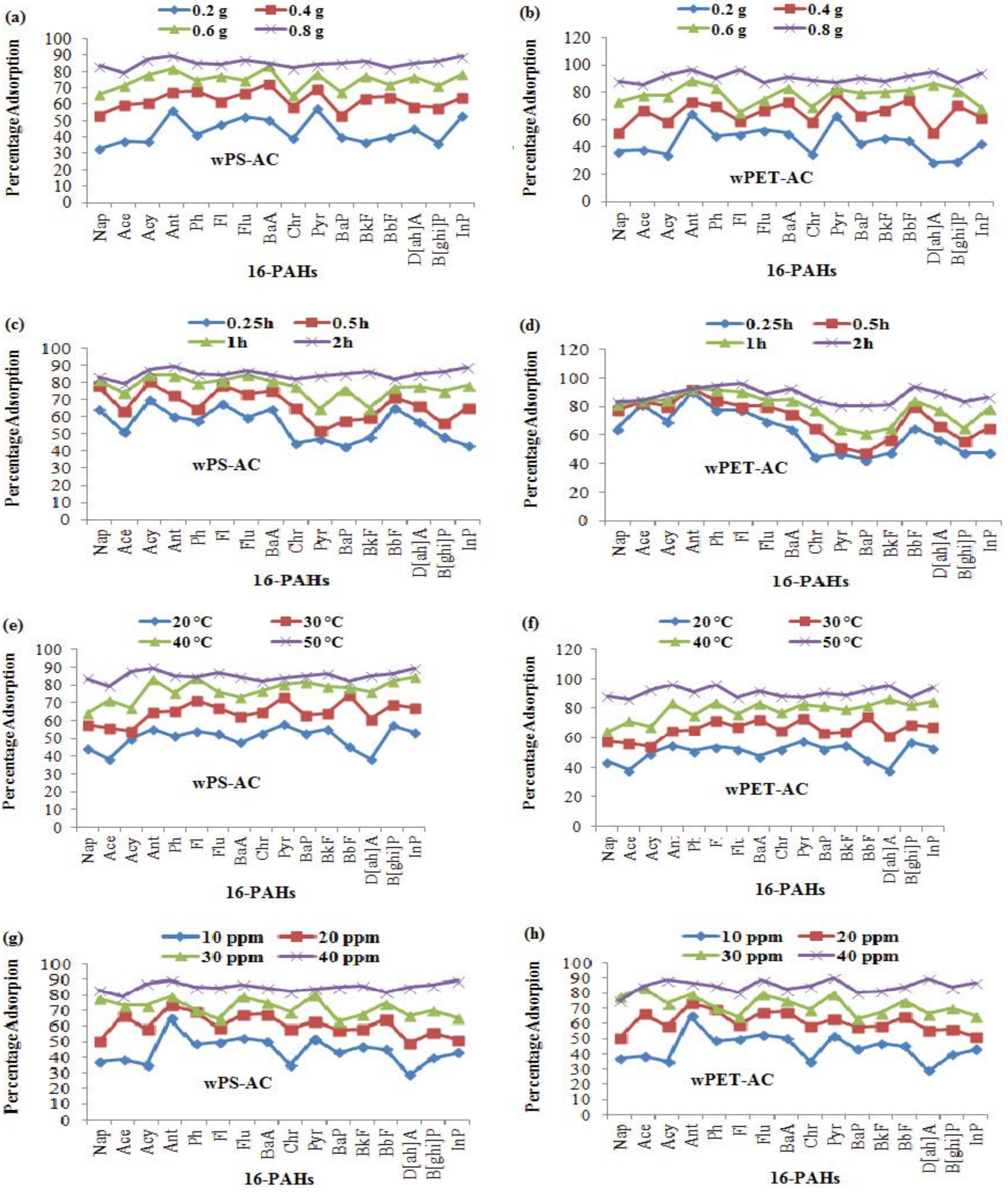

Fig. 2. Removal (%) of PAHs using wPS-AC and wPET-AC under different experimental conditions; (a) and (b) effect of adsorbent dose, (c) and (d) effect of contact time, (e) and (f) effect of temperature, and (g) and (h) effect of initial concentration.

3.2.5. Adsorption kinetics

In the adsorption process, it is said that pseudo-first-order equations and pseudo-second-order kinetic models are used to express the chemical reactions. The most widely used equation in AC adsorption is pseudo-second-order. The estimation of the exploratory adsorption limit ($q_{e,\text{exp}}$) was found to be in acceptable concurrence with determined q_e values ($q_{e,\text{cal}}$) by pseudo-second-order model at all temperatures. Furthermore, the high estimation of the correlation coefficient (R^2) additionally proposes that pseudo-second-order model is better appropriate at all temperatures. Table 5 details the R^2 values, adsorption capacity and rate constants of these two models. The plots of the linearized form of pseudo-second-order model (t/q_t vs. t) are given in Fig. 3. The pseudo-second-order model depends on the presumption that the rate-limiting step may be chemical adsorption, including the valence generated by the exchange or sharing of electrons between the adsorbate and the adsorbent. It provides the best correlation of data. These outcomes are in good agreement with other studies on Nap adsorption by activated carbon [50], sorption of poly-aromatic hydrocarbons onto granular activated carbons [50], desorption studies of 2,4,6-trichlorophenol on oil palm [51], phenols on activated carbon fibers [50], modified coir pith [52], dolomite [53], and $ZnCl_2$ activated coir pith carbon [54].

3.2.6. Isotherm study

Several models in the literature were described using adsorption isotherms [55]. These models are preferred

Table 4
Thermodynamic factors for the adsorption of PAHs onto wPET-AC and wPS-AC

PAHs	wPET-AC			wPS-AC		
	ΔG° (kJ mol^{-1})	ΔH° (kJ mol^{-1})	ΔS° (kJ mol^{-1})	ΔG° (kJ mol^{-1})	ΔH° (kJ mol^{-1})	ΔS° (kJ mol^{-1})
Nap	6.21	–3.41	0.01	6.33	–1.14	0.02
Ace	6.26	–3.41	0.01	6.46	–1.14	0.02
Acy	6.09	–3.41	0.01	6.22	–1.14	0.02
Ant	6.00	–3.41	0.01	6.16	–1.14	0.02
Ph	6.14	–3.41	0.01	6.28	–1.14	0.02
Fl	6.00	–3.41	0.01	6.30	–1.14	0.02
Flu	6.23	–3.41	0.01	6.23	–1.14	0.02
BaA	6.12	–3.41	0.01	6.30	–1.14	0.02
Chr	6.21	–3.41	0.01	6.37	–1.14	0.02
Pyr	6.22	–3.41	0.01	6.32	–1.14	0.02
BaP	6.14	–3.41	0.01	6.29	–1.14	0.02
BkF	6.19	–3.41	0.01	6.26	–1.14	0.02
BbF	6.08	–3.41	0.01	6.37	–1.14	0.02
D[ah]A	6.01	–3.41	0.01	6.29	–1.14	0.02
B[ghi]P	6.22	–3.41	0.01	6.25	–1.14	0.02
InP	6.05	–3.41	0.01	6.17	–1.14	0.02

Table 5
Pseudo-second-order kinetic parameters for adsorption of PAHs over wPET-AC and wPS-AC in batch experiment

PAHs	wPET-AC			wPS-AC		
	k_2 (μg g^{-1} min^{-1})	q_{e2} (μg g^{-1})	R^2	k_2 (μg g^{-1} min^{-1})	q_{e2} (μg g^{-1})	R^2
Nap	1.7×10^{-4}	0.11	0.937	5.0×10^{6}	1.0×10^{2}	0.962
Ace	3.2×10^{-3}	0.52	0.906	3.3×10^{6}	1.0×10^{2}	0.947
Acy	1.6×10^{-4}	0.11	0.865	4.1×10^{4}	1.1×10^{2}	0.932
Ant	1.3×10^{-4}	0.71	0.785	3.3×10^{6}	1.0×10^{2}	0.950
Ph	1.4×10^{-4}	0.10	0.861	1.0×10^{7}	1.0×10^{2}	0.996
Fl	1.0×10^{-4}	0.09	0.943	8.3×10^{8}	9.0×10^{1}	0.999
Flu	1.5×10^{-5}	0.10	0.794	1.0×10^{7}	1.0×10^{2}	0.998
BaA	7.2×10^{-5}	0.07	0.937	8.3×10^{8}	1.0×10^{2}	0.997
Chr	4.8×10^{-5}	0.05	0.861	8.3×10^{8}	9.0×10^{1}	0.996
Pyr	6.4×10^{-5}	0.05	0.988	1.0×10^{7}	1.0×10^{2}	0.987
BaP	6.0×10^{-5}	0.05	0.987	1.2×10^{7}	1.1×10^{2}	0.983
BkF	6.5×10^{-5}	0.06	0.998	1.2×10^{7}	1.1×10^{2}	0.985
BbF	7.4×10^{-5}	0.07	0.898	8.3×10^{7}	9.0×10^{1}	0.998
D[ah]A	6.2×10^{-5}	0.06	0.974	8.3×10^{8}	9.0×10^{1}	0.998
B[ghi]P	5.7×10^{-5}	0.05	0.998	1.0×10^{7}	1.0×10^{2}	0.998
InP	4.7×10^{-5}	0.05	0.907	1.0×10^{7}	1.0×10^{2}	0.998

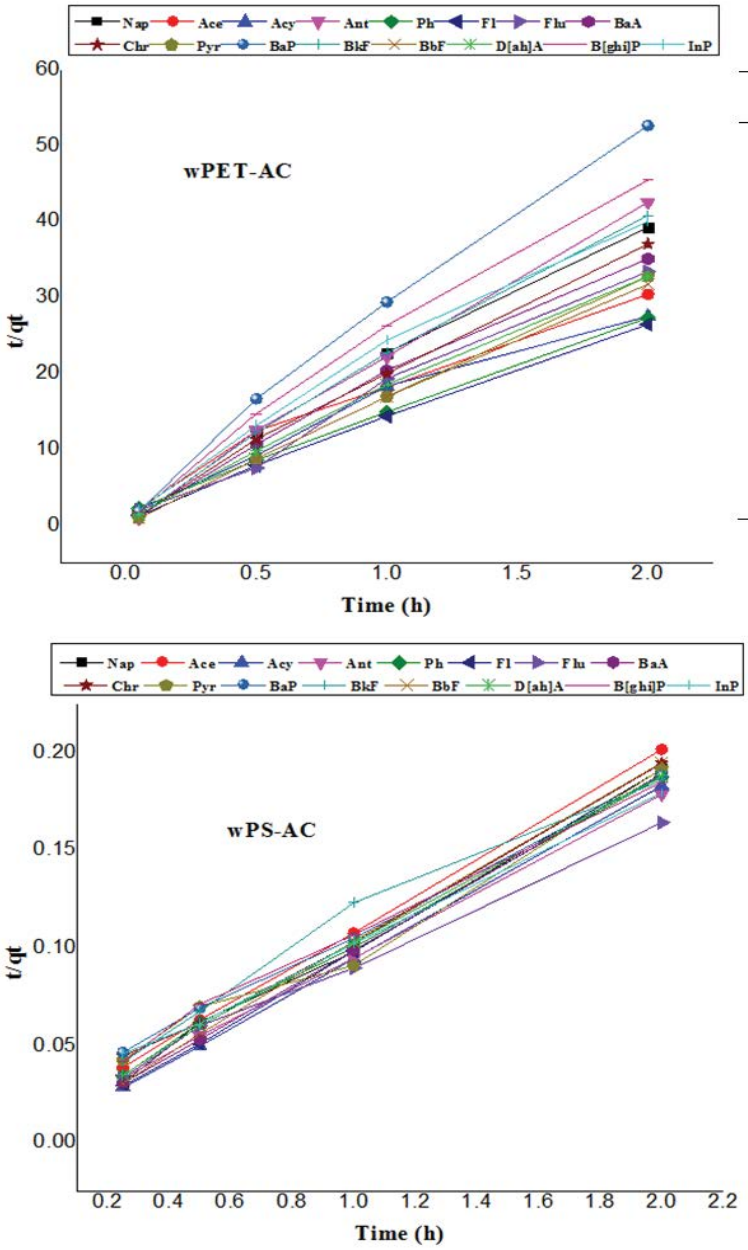

		wPET-AC	
PAHs	**Slope**	**Intercept**	**R^2**
Nap	9.09	5.34×10^{4}	0.937
Ace	1.92	6.00×10^{2}	0.906
Acy	9.09	5.68×10^{4}	0.865
Ant	1.41	1.08×10^{4}	0.785
Ph	10.00	7.14×10^{4}	0.861
Fl	11.11	1.11×10^{4}	0.943
Flu	10.00	6.67×10^{6}	0.794
BaA	14.28	1.98×10^{5}	0.937
Chr	20.00	4.17×10^{5}	0.861
Pyr	20.00	3.12×10^{5}	0.988
BaP	20.00	6.00×10^{-5}	0.987
BkF	16.67	2.56×10^{5}	0.998
BbF	14.28	1.93×10^{5}	0.898
D[ah]A	16.67	2.69×10^{6}	0.974
B[ghi]P	20.00	7.02×10^{6}	0.998
InP	20.00	8.51×10^{6}	0.907

		wPS-AC	
PAHs	**Slope**	**Intercept**	**R^2**
Nap	0.01	2.00×10^{-11}	0.962
Ace	0.01	3.03×10^{-11}	0.947
Acy	0.01	2.02×10^{-09}	0.932
Ant	0.01	3.03×10^{-11}	0.950
Ph	0.01	1.00×10^{-11}	0.996
Fl	0.01	1.49×10^{-13}	0.999
Flu	0.01	1.00×10^{-11}	0.998
BaA	0.01	1.20×10^{-13}	0.997
Chr	0.01	1.49×10^{-13}	0.996
Pyr	0.01	1.00×10^{-11}	0.987
BaP	0.01	6.89×10^{-12}	0.983
BkF	0.01	6.89×10^{-12}	0.985
BbF	0.01	1.49×10^{-12}	0.998
D[ah]A	0.01	1.49×10^{-13}	0.998
B[ghi]P	0.01	1.20×10^{-12}	0.998
InP	0.01	1.00×10^{-11}	0.998

Fig. 3. Plots of the pseudo-second-order kinetics for wPET-AC and wPS-AC in batch experiment.

because of their simplicity and common use. Langmuir and Freundlich models are the most commonly used models [56]. When a perfectly homogeneous adsorption occurs in the adsorption process, the correct Langmuir adsorption data can be yielded. In Freundlich model, it is assumed that the adsorption occurs on the heterogeneous surfaces and can form mono or multilayers depending on the amount of adsorbate adsorbed at equilibrium. It is important to plan a suitable model to describe the best isotherm model for activated carbon adsorption [57]. Data were acquired from the isotherm models applied for clarifying the response between adsorbent and adsorbed Phe and optimizing the amount of adsorbent [56]. Based on the results, Langmuir isotherm models provided the best fit with the experimental data. These results are consistent with the results of different tests performed recently by the adsorption of Phe on activated carbon [41,44,50,57,58]. The determined Langmuir constants (K_1 and q_m) as well as the R^2 for the two isotherms are given in Table 6. Figs. 4 and 5 show the plots of Langmuir isotherms for adsorption of 16-PAHs over wPET-AC and wPS-AC, respectively.

3.3. Mechanisms of PAHs adsorption

In a general sense, the adsorption of pollutants from aqueous phase by AC depends on the surface characteristics of the adsorbent, the nature of the adsorbate, and the solution condition. Various mechanisms by which the carbon

Table 6
Isotherm model parameters for PAHs adsorption over wPET-AC and wPS-AC in batch experiment

PAHs	Langmuir isotherm parameters			Langmuir isotherm parameters		
	wPET-AC			wPS-AC		
	q_m (μg g^{-1})	K_1	R^2	q_m (μg g^{-1})	K_1	R^2
Nap	6.29	0.11	0.965	43.48	2.07 × 10^{-6}	0.950
Ace	7.25	0.04	0.974	34.48	2.32 × 10^{-5}	0.937
Acy	7.04	0.05	0.986	33.33	2.10 × 10^{-5}	0.925
Ant	18.52	0.02	0.988	32.26	3.10 × 10^{-5}	0.928
Ph	8.06	0.01	0.984	50.00	1.20 × 10^{-5}	0.980
Fl	14.92	0.07	0.938	37.04	1.35 × 10^{-5}	0.975
Flu	7.04	0.05	0.990	38.46	1.04 × 10^{-6}	0.954
BaA	43.48	0.05	0.920	34.48	2.90 × 10^{-5}	0.960
Chr	22.73	0.12	0.945	34.48	2.90 × 10^{-5}	0.947
Pyr	25.64	0.07	0.919	45.45	1.98 × 10^{-5}	0.960
BaP	10.30	0.62	0.985	35.71	2.52 × 10^{-5}	0.910
BkF	2.67	0.02	0.996	52.63	1.71 × 10^{-5}	0.969
BbF	7.58	0.02	0.992	41.67	2.16 × 10^{-6}	0.966
D[ah]A	0.02	3.2 × 10^{-5}	0.923	55.56	1.62 × 10^{-6}	0.987
B[ghi]P	0.02	45 × 10^{4}	0.858	47.62	1.89 × 10^{-6}	0.966
InP	0.02	5.8 × 10^{4}	0.922	34.48	2.61 × 10^{-6}	0.942

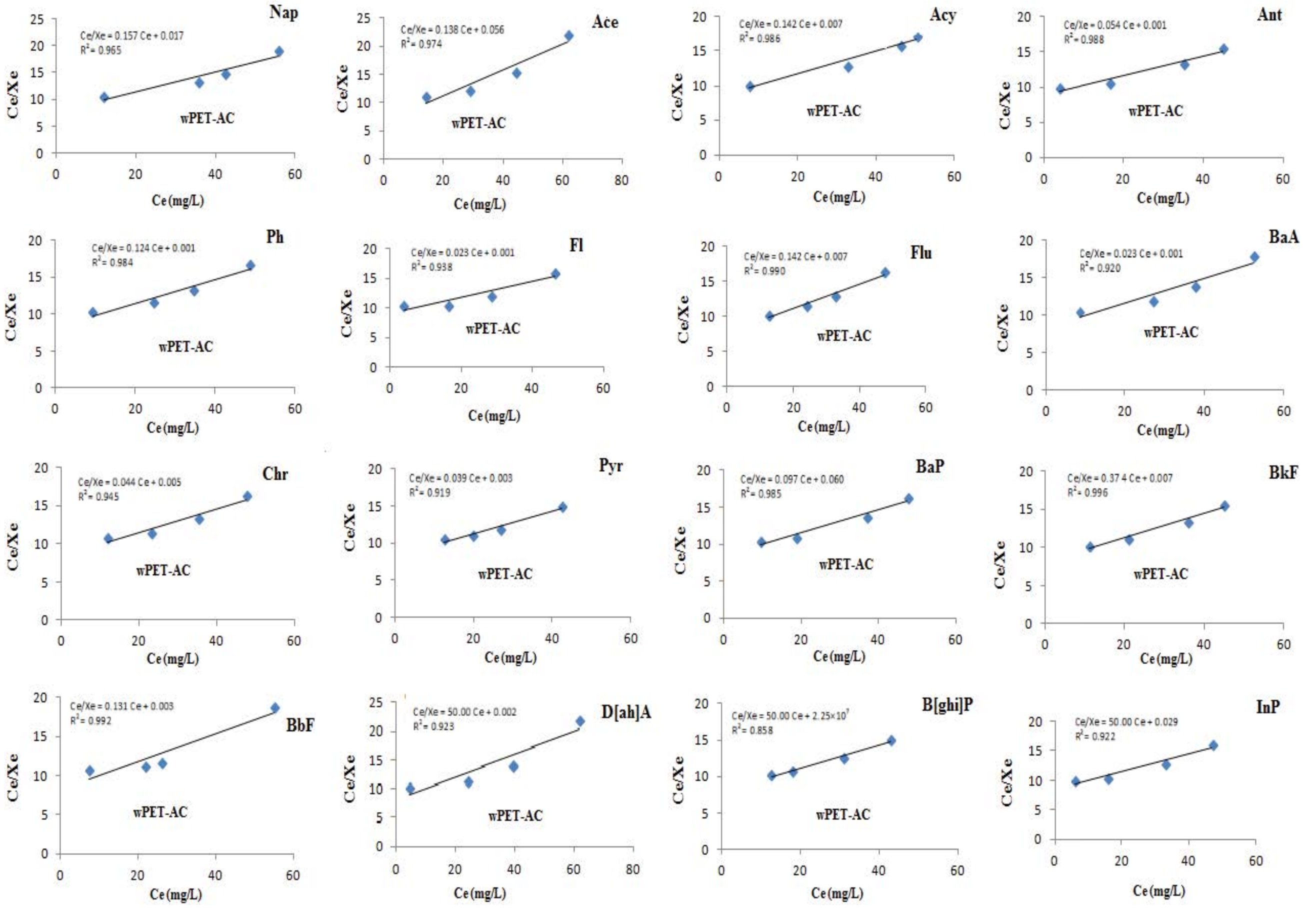

Fig. 4. Plots of Langmuir isotherms for 16-PAHs adsorption over wPET-AC in batch experiment.

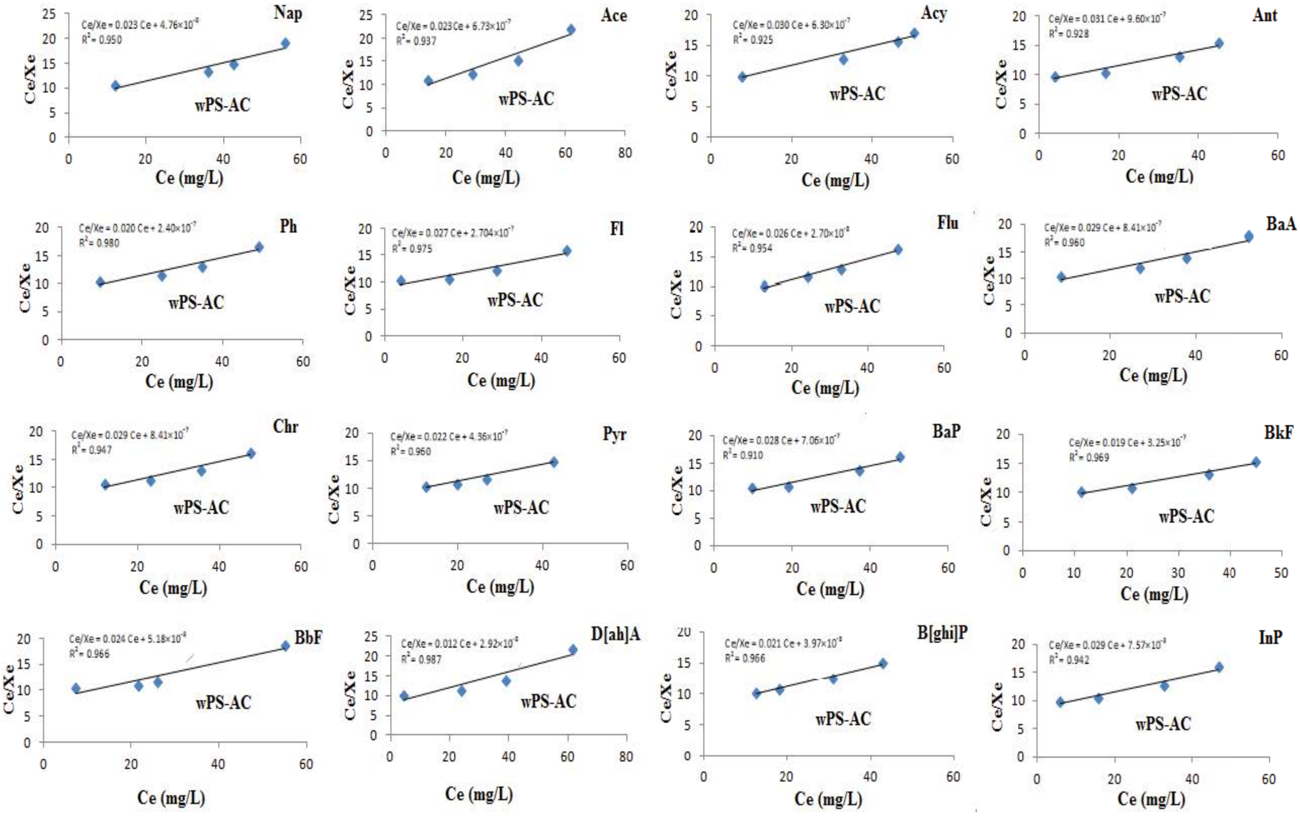

Fig. 5. Plots of Langmuir isotherms for 16-PAHs adsorption over wPS-AC in batch experiment.

surface functional groups might influence the adsorption process from aqueous phase have been proposed: π–π dispersive interactions [59], hydrogen bonding [59,60] and electron–donor–acceptor interactions [61]. For organic pollutants, as is the case of PAHs, Lyklema. [62] noted that their adsorption from solution is essentially an exchange process, and hence molecules adsorb not only because they are attracted by solids but also because the solution may reject them (the hydrophobic effect). The adsorption process of organic compounds on AC surface has thus been described as a complex interplay between electrostatic and dispersive interactions, especially in the case of weak organic electrolytes. However, since PAHs are not considered electrolytic, the van der Waals dispersive interaction and, in some cases, the intermediate hydrogen bonding interaction, has been the dominant mechanism proposed in the literature [63]. The mechanism of adsorption of PAH by AC is given in the reaction scheme (Fig. 6) [64].

3.4. Physical and biochemical characteristics of VWW before and after treatment

Table 7 shows the biochemical and physical characteristics of VWW before and after the treatment process using the newly produced AC from wPS and wPET. The subsequent observations can be concluded from Table 7, as for the biochemical and physical characteristics of VWW samples after the treatment process. The results obtained for pH for the samples were within the range of 6.5–7.5. Outcomes acquired demonstrated that there was a remarkable decrease in the amount of suspended solids, TDS, COD, DO, and BOD_5 after treatment. Trial outcomes from Table 7 demonstrated that the turbidity was relatively removed. The outcomes from Table 5 showed that the AC manufactured from wPS and wPET totally eliminated the offensive odour in the VWW, with a clear appearance.

3.5. Comparison of adsorption potential of different adsorbents

Activated carbon is well known in PAHs sorption due to their high specific surface area (ranging from 300 to 3,000 m^2/g) [61]. Activated carbon is generated from a variety of materials (plant-derived materials, petroleum coke, shells, sewage sludge, as well as bituminous coal) [56] through carbonization and subsequent activation processes. Activated carbon is set up as a briquette, granules, or powder relying upon its particular application. Although, the adsorption of PAHs by powder and granular activated carbon is widespread in practice, granular activated carbon is one of the most commonly used permeable media, which can be used to remove organic contaminants through adsorption measures [65–68]. Table 8 details the different adsorption media reported in the literature and the comparative adsorption efficiency of AC, that is, wPET-AC and wPS-AC) on PAHs adsorption. The wPET-AC and wPS-AC have extraordinary qualities in utilizing PAHs adsorption media because of it re-usability, good settle ability, high adsorption capacity and miscible nature with aqueous solution.

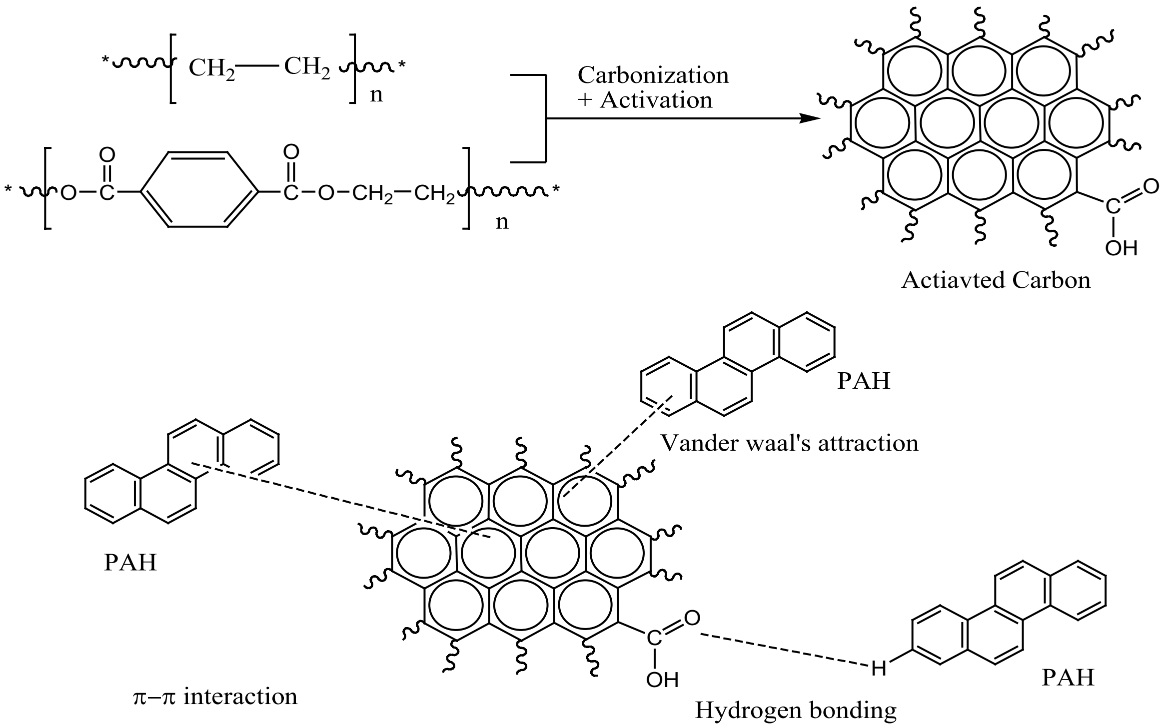

Fig. 6. Reaction scheme: preparation and mechanism of adsorption of AC [64].

Table 7
Physical and biochemical characteristics of vehicle-wash wastewater before and after treatment process

Parameters	Before treatment	Effluent after treatment	
		wPS-AC	wPET-AC
pH	6.67	7.20	7.05
Suspended solids (mg/L)	100	15	5
TDS (mg/L)	637	410	179
COD (mg/L)	378	142	152
DO (mg/L)	4.90	2.17	1.05
BOD_5 (mg/L)	415	110	77
Turbidity (NTU)	62	0	0
Appearance	Not clear	Clear	Clear
Odour	Offensive	Totally removed	Totally removed

4. Conclusions

PAHs could be removed from aqueous solution as well as wastewater by means of various types of adsorbents, for example, membranes, cellulose, sediments, sand, amended clay, organic minerals, biochar and activated carbon. The capability of the sorption process depends not just on the characteristics of the adsorbate with the adsorbent, yet in addition on the working factors. In the present work, the activated char wPET-AC and wPS-AC were synthesized by an economical and simple method. The synthesized chars were effectively used for the removal of PAHs from VWW. The removal process is totally dependent on the initial PAHs concentration, contact time, temperature, adsorbent dose, adsorbent bed height, and flow rate. The removal process proceeded and fitted with Langmuir and Freundlich isotherms and pseudo-second-order equations. Thermodynamic calculations indicated that the adsorption process is exothermic and nonspontaneous in nature. This study recommends that wPET-AC and wPS-AC can be utilized as appropriate and productive adsorbents in the expulsion of PAHs as of aqueous solutions in addition to VWW.

Research funding

The authors acknowledge the funding offered by University of Peshawar, Khyber Pakhtunkhwa, Pakistan.

Table 8
Details of various adsorption media and their PAHs removal effectiveness

Materials	Study type	PAHs % removal effectiveness	Sorption isotherm model	References
Aspen wood fibre	Batch/Column	Pyr (74), Ant (67), Fl (25.5)	Freundlich	[52]
Activated carbon	Batch	>97% Nap and >98% Flu	Langmuir and Freundlich,	[58]
Coke-derived porous carbon	Batch	Nap, Fl, Ph, Pyr, Flu (>99 for all PAHs)	Freundlich	[60]
Wood char	Batch	Pyr, Ph, BaA (≥60)	Freundlich	[69]
Inorgano–organo-bentonite	Batch	Ph (99)	Langmuir	[70]
Powder activated carbon anthracite based and coconut shells based	Batch	BbF (86), Ph (95), Chr (94.5), BaP (88), Flu (96.5), Pyr (98), BaA (94.5), InP (73), BkF (88), B[g,h,i]P (69), Ant (97.5)	Freundlich	[71]
Wood ashes	Batch	B[ghi]P,Fl, Pyr, BaP, Cry, BaA, BbF, D[ah]A, BkF, InP (>99)	Freundlich	[72]
wPS-AC	Batch/Column	Nap (90.61), Ace (89.40), Acy (92.50), Ant (94.64), Ph (95.33), Fl (94.66), Flu (96.02), BaA (94.7), Chr (92.3), Pyr (94.10), BaP (95.07), BkF (96.23), BbF (92.15), D[ah]A (90.01), B[ghi]P (96.54), InP (93.25)	Langmuir and Freundlich,	This article
wPET-AC	Batch/Column	Nap (96.22), Ace (94.67), Acy (97.21), Ant (98.22), Ph (93.65), Fl (97.31), Flu (94.02), BaA (92.10), Chr (90.31), Pyr (93.46), BaP (92.23), BkF (93.25), BbF (94.49), D[ah]A (95.09), B[ghi]P (91.54), InP (96.47)	Langmuir and Freundlich,	This article

Conflict of interest

Authors state no conflict of interest.

Informed consent

Informed consent is not applicable.

Ethical approval

The conducted research is not related to either human or animal use.

References

[1] A.O. Adeniji, O.O. Okoh, A.I. Okoh, Analytical methods for polycyclic aromatic hydrocarbons and their global trend of distribution in water and sediment: a review, Recent insights in petroleum science and engineering, 10 (2018). ISBN: 978-953-51-5321-4. https://doi.org/10.5772/intechopen.71163.

[2] S.R. Wild, K.C. Jones, Polynuclear aromatic hydrocarbons in the United Kingdom environment: a preliminary source inventory and budget, Environ. Pollut., 88 (1995) 91–108.

[3] B. Kumar, V.K. Verma, C.S. Sharma, A.B. Akolkar, Estimation of toxicity equivalency and probabilistic health risk on lifetime daily intake of polycyclic aromatic hydrocarbons from urban residential soils, Hum. Ecol. Risk Assess., 21 (2015) 434–444.

[4] Y. Zhang, S. Tao, Global atmospheric emission inventory of polycyclic aromatic hydrocarbons (PAHs) for 2004, Atmos. Environ., 43 (2009) 812–819.

[5] M. Brazkova, A. Krastanov, Polycyclic aromatic hydrocarbons: sources, effects and biodegradation, Научни Трудове На Русенския Университет, Том., 10 (2013) 1.

[6] R.C. Sims, M.R. Overcash, Fate of Polynuclear Aromatic Compounds (PNAs) in Soil-Plant Systems, In Residue Reviews, Springer, New York, NY, 1983, pp. 1–68.

[7] E. Manoli, C. Samara, Polycyclic aromatic hydrocarbons in natural waters: sources, occurrence and analysis, TrAC-Trends Anal. Chem., 18 (1999) 417–428.

[8] K. Ravindra, R. Sokhi, G.R. Van, Atmospheric polycyclic aromatic hydrocarbons: source attribution, emission factors and regulation, Atmos. Environ., 42 (2008) 2895–2921.

[9] R. Eisler, Mercury Hazards to Fish, Wildlife, and Invertebrates: A Synoptic Review (No. 10), Fish and Wildlife Service, US Department of the Interior, 1987.

[10] USEPA, National Center for Environmental Assessment, Office of Research and Development, Washington, DC, 2008.

[11] J. Xu, D.L. Sparks, Molecular Environmental Soil Science, Springer Netherlands, 2013.

[12] J. Masih, R. Singhvi, K. Kumar, V.K. Jain, A. Taneja, Seasonal variation and sources of polycyclic aromatic hydrocarbons (PAHs) in indoor and outdoor air in a semi arid tract of northern India, Aerosol Air Qual. Res., 12 (2012) 515–525.

[13] M. Akyüz, H. Çabuk, Gas–particle partitioning and seasonal variation of polycyclic aromatic hydrocarbons in the atmosphere of Zonguldak, Turkey, Sci. Total Environ., 408 (2010) 5550–5558.

[14] C.D. Klaassen, M.O. Amdur, Casarett and Doull's Toxicology: the Basic Science of Poisons, McGraw-Hill, New York, Vol. 1236, 2013, p. 189.

[15] H.I. Abdel-Shafy, M.S. Mansour, A review on polycyclic aromatic hydrocarbons: source, environmental impact, effect on human health and remediation, Egypt. J. Petrol., 25 (2016) 107–123.

[16] B. Chen, D. Zhou, L. Zhu, Transitional adsorption and partition of nonpolar and polar aromatic contaminants by biochars of pine needles with different pyrolytic temperatures, Environ. Sci. Technol., 42 (2008) 5137–5143.

[17] S. Lamichhane, K.B. Krishna, R. Sarukkalige, Polycyclic aromatic hydrocarbons (PAHs) removal by sorption: a review, Chemosphere, 148 (2016) 336–353.

[18] K.L. Shih, J. Lederberg, Chloramine mutagenesis in *Bacillus subtilis*, Science, 192 (1976) 1141–1143.

[19] M. Ilyas, W. Ahmad, H. Khan, I. Ahmad, Application of composite adsorbents prepared from waste PS and PET for removal of Cr and Cu ions from wastewater, Desal. Wat. Treat., 171 (2019) 144–157.

[20] C.S. Umpierres, P.S. Thue, E.C. Lima, G.S.D. Reis, I.A. de Brum, W.S.D. Alencar, S.L. Dias, G.L. Dotto, Microwave-activated carbons from tucumã (*Astrocaryum aculeatum*) seed for efficient removal of 2-nitrophenol from aqueous solutions, Environ. Technol., 39 (2018) 1173–1187.

[21] M. Ilyas, W. Ahmad, H. Khan, S. Yousaf, Potentially poisonous elements removal from vehicle-wash wastewater and aqueous solutions using composite adsorbents, Desal. Wat. Treat., 224 (2021) 331–342.

[22] A. Mittal, R. Ahmad, I. Hasan, Biosorption of Pb2+, Ni2+ and Cu2+ ions from aqueous solutions by L-cystein-modified montmorillonite-immobilized alginate nanocomposite, Desal. Wat. Treat., 57 (2016) 17790–17807.

[23] A. Mittal, R, Ahmad, I. Hasan, Poly(methyl methacrylate)-grafted alginate/Fe3O4 nanocomposite: synthesis and its application for the removal of heavy metal ions, Desal. Water Treat., 57 (2016) 19820–19833.

[24] N.M. Alandis, W. Mekhamer, O. Aldayel, J.A.A. Hefne, M. Alam, Adsorptive applications of montmorillonite clay for the removal of Ag(I) and Cu(II) from aqueous medium, J. Chem., 2019 (2019) 1–7.

[25] C. Vanlalveni, S. Lallianrawna, A. Biswas, M. Selvaraj, B. Changmai, S.L. Rokhum, Green synthesis of silver nanoparticles using plant extracts and their antimicrobial activities: a review of recent literature, RSC Adv., 11 (2016) 2804–2837.

[26] A. Mittal, R. Ahmad, I. Hasan, Iron oxide-impregnated dextrin nanocomposite: synthesis and its application for the biosorption of Cr (VI) ions from aqueous solution, Desal. Wat. Treat., 57 (2016) 15133–15145.

[27] J. Mittal, R. Ahmad, A. Mariyam, V.K. Gupta, A. Mittal, Expeditious and enhanced sequestration of heavy metal ions from aqueous environment by papaya peel carbon: a green and low-cost adsorbent, Desal. Wat. Treat., 210 (2021) 365–376.

[28] R. Ahmad, I. Hasan, A. Mittal, Adsorption of Cr (VI) and Cd (II) on chitosan grafted polyaniline-OMMT nanocomposite: isotherms, kinetics and thermodynamics studies, Desal. Wat. Treat., 58 (2017) 144–153.

[29] H. Daraei, A. Mittal, Investigation of adsorption performance of activated carbon prepared from waste tire for the removal of methylene blue dye from wastewater, Desal. Wat. Treat., 90 (2017) 294–298.

[30] S. Soni, P.K. Bajpai, D. Bharti, J. Mittal, C. Arora, Removal of crystal violet from aqueous solution using iron based metal organic framework, Desal. Wat. Treat., 205 (2020) 386–399.

[31] R. Jain, P. Sharma, S. Sikarwar, J. Mittal, D. Pathak, Adsorption kinetics and thermodynamics of hazardous dye Tropaeoline 000 unto Aeroxide Alu C (Nano alumina): a non-carbon adsorbent, Desal. Wat. Treat., 52 (2014) 7776–7783.

[32] I. Anastopoulos, I. Pashalidis, A.G. Orfanos, I.D. Manariotis, T. Tatarchuk, L. Sellaoui, A. Bonilla-Petriciolet, A. Mittal, A. Núñez-Delgado, Removal of caffeine, nicotine and amoxicillin from (waste) waters by various adsorbents. A review, J. Environ. Manage., 261 (2020) 110236.

[33] S. Soni, P.K. Bajpai, J. Mittal, C. Arora, Utilisation of cobalt doped Iron based MOF for enhanced removal and recovery of methylene blue dye from waste water, J. Mol. Liq., 314 (2020) 113642.

[34] D. Pan, S. Ge, J. Zhao, J. Tian, Q. Shao, L. Guo, X. Mai, T. Wu, V. Murugadoss, H. Liu, T. Ding, Synthesis and characterization of ZnNiIn layered double hydroxides derived mixed metal oxides with highly efficient photoelectrocatalytic activities, Ind. Eng. Chem. Res., 58 (2018) 836–848.

[35] J. Mittal, A. Mittal, Hen Feather, A Remarkable Adsorbent for Dye Removal. Green Chemistry for Dyes Removal from Wastewater, Scrivener Publishing LLC, USA, 2015, pp. 409–457.

[36] Y. Hu, Y. He, X. Wang, C. Wei, Efficient adsorption of phenanthrene by simply synthesized hydrophobic MCM-41 molecular sieves, Appl. Surf. Sci., 311 (2014) 825–830.

[37] J. Liu, J. Chen, L. Jiang, X. Yin, Adsorption of mixed polycyclic aromatic hydrocarbons in surfactant solutions by activated carbon, J. Ind. Eng. Chem., 20 (2014) 616–623.

[38] F. Lian, B. Xing, L. Zhu, Comparative study on composition, structure, and adsorption behavior of activated carbons derived from different synthetic waste polymers, J. Colloid Interface Sci., 360 (2011) 725–730.

[39] Y.S. Ho, G. McKay, Sorption of dye from aqueous solution by peat, Chem. Eng. J., 70 (1998) 115–124.

[40] S. Chen, J. Zhang, C. Zhang, Q. Yue, Y. Li, C. Li, Equilibrium and kinetic studies of methyl orange and methyl violet adsorption on activated carbon derived from *Phragmites australis*, Desalination, 252 (2010) 149–156.

[41] Y. Yao, B. Gao, J. Fang, M. Zhang, H. Chen, Y. Zhou, A.E. Creamer, Y. Sun, L. Yang, Characterization and environmental applications of clay–biochar composites, Chem. Eng. J., 242 (2014) 136–143.

[42] M. Lawrinenko, D.A. Laird, Anion exchange capacity of biochar, Green Chem., 17 (2015) 4628–4636.

[43] E. Mansouri, V. Yousefi, V. Ebrahimi, S. Eyvazi, M.S. Hejazi, M. Mahdavi, M. Asghar, V. Tarhriz, Overview of ultraviolet-based methods used in polycyclic aromatic hydrocarbons analysis and measurement, Sep. Sci., 3 (2020) 112–120.

[44] M. Ilyas, W. Ahmad, H. Khan, S. Yousaf, M. Yasir, A. Khan, Environmental and health impacts of industrial wastewater effluents in Pakistan: a review, Rev. Environ. Health, 34 (2019) 171–186.

[45] M.N. Zafar, R. Nadeem, M.A. Hanif, Biosorption of nickel from protonated rice bran, J. Hazard. Mater., 143 (2007) 478–485.

[46] S. Athapaththu, A Comprehensive Study of Cd(II) Removal From Aqueous Solution Via Adsorption and Solar Photocatalysis, Electronic Thesis and Dissertation Repository, Vol. 19, 2013, p. 1783.

[47] K.G. Bhattacharyya, S.S. Gupta, Kaolinite, montmorillonite, and their modified derivatives as adsorbents for removal of Cu (II) from aqueous solution, Sep. Purif. Technol., 50 (2006) 388–397.

[48] W. Konicki, I. Pełech, E. Mijowska, I. Jasińska, Adsorption of anionic dye Direct Red 23 onto magnetic multi-walled carbon nanotubes-Fe3C nanocomposite: kinetics, equilibrium and thermodynamics, Chem. Eng. J., 210 (2012) 87–95.

[49] F.A. Dawodu, K.G. Akpomie, Simultaneous adsorption of Ni (II) and Mn (II) ions from aqueous solution unto a Nigerian kaolinite clay, J. Mater. Res. Technol., 3 (2014) 129–141.

[50] Q.S. Liu, T. Zheng, P. Wang, J.P. Jiang, N. Li, Adsorption isotherm, kinetic and mechanism studies of some substituted phenols on activated carbon fibers, Chem. Eng. J., 157 (2010) 348–356.

[51] K.A. Krishnan, A. Haridas, Removal of phosphate from aqueous solutions and sewage using natural and surface modified coir pith, J. Hazard. Mater., 152 (2008) 527–535.

[52] T.B. Boving, W. Zhang, Removal of aqueous-phase polynuclear aromatic hydrocarbons using aspen wood fibers, Chemosphere, 54 (2004) 831–839.

[53] C. Namasivayam, D. Sangeetha, Equilibrium and kinetic studies of adsorption of phosphate onto $ZnCl_2$ activated coir pith carbon, J. Colloid Interface Sci., 280 (2004) 359–365.

[54] B.H. Hameed, Evaluation of papaya seeds as a novel non-conventional low-cost adsorbent for removal of methylene blue, J. Hazard. Mater., 162 (2009) 939–944.

[55] V. Srihari, A. Das, Comparative studies on adsorptive removal of phenol by three agro-based carbons: equilibrium and isotherm studies, Ecotox. Environ. Saf., 71 (2008) 274–283.

[56] B. Özkaya, Adsorption and desorption of phenol on activated carbon and a comparison of isotherm models, J. Hazard. Mater., 129 (2006) 158–163.

[57] C.O. Ania, B. Cabal, J.B. Parra, A. Arenillas, B. Arias, J.J. Pis, Naphthalene adsorption on activated carbons using solvents of different polarity, J. Adsorpt., 14 (2008) 343–355.

[58] A. Awoyemi, Understanding the Adsorption of Polycyclic Aromatic Hydrocarbons from Aqueous Phase onto Activated Carbon (Doctoral dissertation), 2011, pp. 1–135.

[59] R. Coughlin, F.S. Ezra, Role of surface acidity in the adsorption of organic pollutants on the surface of carbon, Environ. Sci. Technol., 2 (1968) 291–297.

[60] M. Yuan, S. Tong, S. Zhao, C.Q. Jia, Adsorption of polycyclic aromatic hydrocarbons from water using petroleum coke-derived porous carbon, J. Hazard. Mater., 181 (2010) 1115–1120.

[61] J.S. Mattson, H.B. Mark Jr, M.D. Malbin, W.B. Weber Jr, J.C. Crittenden, Surface chemistry of active carbon: specific adsorption of phenols, J. Colloid. Interface. Sci., 31 (1968) 116–130.

[62] J. Lyklema, Fundamentals of Interface and Colloid Science. Solid–Liquid Interfaces, Academic Press, New York, Vol. II, 1995, p. 770.

[63] H. Gupta, Removal of phenanthrene from water using activated carbon developed from orange rind, Int. J. Sci. Res. Environ. Sci., 3 (2015) 248.

[64] M. Ilyas, W. Ahmad, H. Khan, Utilization of activated carbon derived from waste plastic for decontamination of polycyclic aromatic hydrocarbons laden wastewater, Water Sci. Technol., 84 (2021) 609–631.

[65] C. Valderrama, J.L. Cortina, A. Farran, X. Gamisans, C. Lao, Kinetics of sorption of polyaromatic hydrocarbons onto granular activated carbon and Macronet hyper-cross-linked polymers (MN200), J. Colloid. Interface Sci., 310 (2007) 35–46.

[66] B. Cabal, C.O. Ania, J.B. Parra, J.J. Pis, Kinetics of naphthalene adsorption on an activated carbon: comparison between aqueous and organic media, Chemosphere, 76 (2009) 433–438.

[67] M. Yuan, S. Tong, S. Zhao, C.Q. Jia, Adsorption of polycyclic aromatic hydrocarbons from water using petroleum coke-derived porous carbon, J. Hazard. Mater., 181 (2010) 1115–1120.

[68] C.O. Ania, B. Cabal, C. Pevida, A. Arenillas, J.B. Parra, F. Rubiera, J.J. Pis, Effects of activated carbon properties on the adsorption of naphthalene from aqueous solutions, J. Appl. Surf. Sci., 253 (2007) 5741–5746.

[69] W. Xilong, T. Sato, B. Xing, Competitive sorption of pyrene on wood chars, Environ. Sci. technol., 40 (2006) 3267–3272.

[70] M. Jianfeng, L. Zhu, Simultaneous sorption of phosphate and phenanthrene to inorgano–organo-bentonite from water, J. Hazard. Mater., 136 (2006) 982–988.

[71] K. Amstaetter, E. Eek, G. Cornelissen, Sorption of PAHs and PCBs to activated carbon: coal versus biomass-based quality, Chemosphere, 87 (2012) 573–578.

[72] M.R. Pérez-Gregorio, M.S. García-Falcón, E. Martínez-Carballo, J. Simal-Gándara, Removal of polycyclic aromatic hydrocarbons from organic solvents by ashes wastes, J. Hazard. Mater., 178 (2010) 273–281.